energy&fuels

Article

pubs.acs.org/EF

# Adjustment of the Biodiesel Free Fatty Acids Content by Means of Adsorption

Debora L. Manuale, Gerardo C. Torres, Juan M. Badano, Carlos R. Vera,* and Juan C. Yori

Instituto de Investigaciones en Catálisis y Petroquímica − INCAPE (FIQ-UNL, CONICET), Santiago del Estero 2654, 3000 Santa Fe, Argentina

**ABSTRACT:** The elimination of free fatty acids (FFAs) and water from biodiesel is usually performed in industrial practice using different units for neutralization with caustic, washing, and drying of the fuel. Adjustment of the acidity, however, can be performed in only one operation using bleaching tanks and commercial adsorbents. The current article explores the use of several adsorbents (TriSyl commercial silicas, diatomaceous earth, impregnated activated carbon) and varying process conditions (temperatures, vacuum levels, residence times) for the removal of FFAs from commercial biodiesel fuel. It was found that silica TriSyl 3000 was the best performing adsorbent, with a capacity for the removal of FFAs of about 1 g $g^{-1}$ at high values of biodiesel acidity. The two factors influencing the capacity for FFA adsorption are the temperature and the silica residual water content. The latter depends on both the temperature and especially the vacuum level of the pretreatment step. The FFA uptakes over TriSyl silicas in a vacuum were 3−4 times larger than that obtained at atmospheric pressure. The adsorption curves were linear in the range of interest (0−2% acidity), and hence, Henry's law could be used. Values of the Henry's constant of 30.0−47.6 (dimensionless) were measured for TriSyl 3000 silica, along with a heat of adsorption of −5.7 kcal $mol^{-1}$. From the kinetic point of view, FFA adsorption is rather slow despite the small diameter of the particles used. The system was found to be highly constrained either by intrinsic slow kinetics or by intraparticle mass-transfer resistance. An unfavorable adsorption equilibrium leading to high adsorbent consumption in one-bleacher operation suggested the use of a countercurrent liquid−solid mode of operation with multiple bleachers. Simulation of two and three serial bleachers working in countercurrent mode revealed that savings greater than 60% can be obtained by using three bleachers operating in countercurrent flow.

## 1. INTRODUCTION

Biodiesel production has increased in the past several years in both developed and developing countries to achieve outstanding levels of installed capacity and annual throughput. Much of this success has been related to the technical maturity of biodiesel production technology and the availability of suppliers of turnkey plants. Most of these plants rely on the alkali-catalyzed transesterification of oils with methanol.[1] This technology can process only feedstocks with low levels of impurities.[2−4] In particular, the presence of free fatty acids (FFAs) is deleterious to the alkaline catalysts and the process.[5] Soaps are formed in the reactor, and the effective concentration of catalyst is reduced. Soaps also form deposits in pipes and vessels that can plug the process lines. This last effect is seen in phase separation units where the presence of these amphiphilic substances disrupts the clean separation of organic and polar phases.

For the treatment of high-acidity oils, intensive feedstock pretreatment is needed, or other reaction technologies have to be used. The higher the content of FFAs in the feedstock, the higher the amount of neutralization needed, and the higher the losses. One alternative is to esterify the FFAs in the presence of an acid catalyst. Acid-catalyzed processes are less popular than alkali-catalyzed techniques because the kinetics are very slow and large reactors are needed.[6] Another possibility is the use noncatalytic reactors employing supercritical methanol. This technology has reached maturity in the past few years, but no industrial application has been reported, except for pilot plants in Japan and Europe.

One important problem in the refining of biodiesel produced in acid-catalyzed and supercritical processes is the adjustment of the acidity of the biodiesel product. Manuale et al.[7] and Anitescu et al.[8] reported that biodiesel produced by reacting supercritical methanol had a residual FFA content of 1−3%. The standard solution for adjusting the acidity of biodiesel could be neutralizing the FFAs and washing away the formed soapstock. This option generates a sizable amount of process wastewater, as pointed out by Karaosmanoglu et al.[9]

Another problem is that of reducing the amount of water.[10] Dehydration of the original fatty feedstock is necessary in the alkaline process to prevent the formation of aqueous sodium hydroxide that transforms the triglycerides into soaps. Dehydration in the acid-catalyzed process is necessary to prevent the deactivation of the catalyst (mineral acid). Conversely, the supercritical process is water-tolerant, and no stringent pretreatment of the feedstock is needed. The process can accommodate feedstocks with medium to high FFA and water contents.

In both the supercritical and classical catalyzed processes, some of the water emerging from the esterification reactor might not be present originally in the feed but might be produced in the same process, as FFA esterification produces esters and water. However, the most important source of water is the washing step needed for the removal of soaps and

**Received:** July 22, 2013
**Revised:** October 10, 2013
**Published:** October 11, 2013





dx.doi.org/10.1021/ef401410v | *Energy Fuels* 2013, 27, 6763−6772

catalysts. In this sense, biodiesel affinity for water is high: water is absorbed during washing and also during storage because of contact with room humidity.

This work addresses the adjustment of the content of FFAs in raw biodiesel by adsorption over several materials. Diatomaceous earth, activated carbon, and silica are studied as disposable bleaching media. Other materials reported as potential FFA adsorbents, such as magnesium silicate[11] and ion exchange resins,[12] were not considered mainly because of their costs.

The emphasis is on finding the optimal bleaching conditions for biodiesel obtained from supercritical reactors. In this sense, the use of noncatalytic reactors for the reaction and adsorption units for refining would lead to a completely "dry" process with no generation of wastewater. The effects of many variables are assessed, including vacuum level, adsorption temperature, and type of adsorbent. The obtained information is rationalized and analyzed with a focus on the utilization of this technique in industrial stirred-tank bleachers. Single and serial bleachers are modeled, to determine whether diffusion or kinetic constraints are high enough to force the use of solid−liquid countercurrent operation for higher adsorbent utilization.

The experimental results of this work were originated in a doctoral thesis by Manuale[13] and are a continuation of our studies on biodiesel refining by adsorptive methods.[14]

## 2. EXPERIMENTAL SECTION

**2.1. Materials.** The raw material employed to produce biodiesel was a refined commercial edible oil (COTO CICSA, soy base, 0.14% FFAs, 500 ppm water). Methanol (99.9%) was supplied by Sintorgan, and oleic acid (>95%) was provided by Indioquímica SA.

The activated carbon employed was a steam-activated bituminous coal in powder form from Calgon Carbon (Filtrasorb 600, 12 × 40 mesh, 1020 minimum iodine number, 2% humidity, 23% ash content). This carbon was further impregnated with magnesium chloride hexahydrate as described elsewhere.[15] Samples are denoted as virgin activated carbon (VAC) and impregnated activated carbon (IAC). Diatomaceous earth (DE) was food-grade Celite 520 (10% retention at 150 mesh, 2.15 g $cm^{-3}$, 6.0-$\mu$m average pore size, 0.80 d'Arcys permeability). Silica samples were TriSyl 3000, 300B, and 450 (Grace Co. Inc., 200 mesh).

**2.2. Biodiesel Preparation.** The transesterification reactions were performed in batch mode using the supercritical method. Twenty-five grams of oil was put into a stainless steel autoclave (50-mm i.d., 100-mm height) with an adjusted volume of methanol to give a molar methanol-to-oil ratio ($R$) of 20. After being charged, the autoclave was purged with nitrogen. Then, the reactor flange was bolted, and the temperature was raised from room temperature to 280 °C and held at this value for 1 h. There were no pressure controls, and the absolute pressure was autogenous. The pressure was measured with a stainless steel bourdon on top of the reactor flange. When the reaction time had been reached, the heating was discontinued, and the reaction was quenched by dipping the autoclave in an ice bath. Excess methanol was then removed from the biodiesel−methanol solution in an atmospheric distillation unit. More details about the experimental setup and conditions can be found elsewhere.[7,16]

Many batches of biodiesel were synthesized and mixed together to provide a common biodiesel stock. The main properties of the biodiesel stock product are reported in Table 1. This biodiesel was kept in a desiccator before use and tested for both FFA and water contents before each experiment. For some experiments (kinetic tests, adsorption isotherms), it was convenient to have samples with higher FFA contents. In these cases, the stock sample was acidified with oleic acid (Matsol 308, Materia Hnos SA) to a value of 1.5−2.5% FFA.

**Table 1. Main Properties of the Biodiesel Base Stock**

| property | normal limits[a] | experimental values |
|---|---|---|
| flash point (°C) | ≥130 | >200 |
| cloud point (°C) | − | 3.2 |
| water (ppm) | ≤500 | 450 |
| viscosity at 40 °C(cSt) | 1.9−6.0 | 5.5 |
| Conradson carbon (mass %) | ≤0.05 | 0.02 |
| cetane index | ≥47 | 55.9 |
| density (g $cm^{-3}$) | 0.87−0.89 | 0.876 |
| FFA (%, g of oleic acid per 100 g) | ≤0.27 | 1.5 |
| sulfated ash (mass %) | ≤0.02 | 0.015 |
| glycerol free/total (mass %) | ≤0.02/≤0.24 | 0.02/0.2 |
| methanol (mass %) | ≤0.2 | 0.15 |

[a]As specified by the ASTM D 6751 and EN 14214 quality standards.

**2.3. Bleaching Experiments.** Both the biodiesel stock batch and the acidified sample were refined by performing bleaching tests at varying conditions and with different adsorbents. Bleaching was performed at 70, 90, and 110 °C in a gas-tight stirred autoclave. Variable adsorbent loadings and contact times of 10−720 min were used. Activated carbon, diatomaceous earth, and silica gel were used as adsorbents.

The effects of vacuum and temperature were assessed by performing the bleaching procedure at normal pressure and in vacuo (160 mmHg) and by varying the reactor temperature (70, 90, and 110 °C). After each treatment, the adsorbents were decanted, and the liquid phase was sampled for analysis.

**2.4. Adsorption Kinetics.** Simple tests were performed to determine approximate adsorption rate equations. In general, the same procedure as used for the bleaching tests was employed, but sampling was performed at different bleaching times. The amount of adsorbate on the solid, $Q$ (expressed in grams of adsorbed oleic acid per 100 g of adsorbent), was determined from a balance of FFAs in the liquid solution taking oleic acid as a model molecule for all calculations.

**2.5. FFA Measurement.** Acidity was determined by means of the colorimetric titration method (ASTM D664). The results are expressed in terms of weight percentage (grams of equivalent oleic acid per 100 g of biodiesel). Solvents and reactants were supplied by different vendors: isopropanol (Ciccarelli, 99.5%), toluene (Merck, 99.9%), sodium hydroxide (Merck, 99.95%), bromothymol blue (Sigma-Aldrich, 95% dye content), and distilled water.

**2.6. Water Content Measurement.** The water contents of the methanol-stripped biodiesel and the bleached biodiesel samples were determined by Karl Fischer potentiometric titration, according to the EN ISO 12937 standard and using reagents supplied by Merck. The titration was performed with an Altronix apparatus with a glass electrode.

**2.7. Biodiesel Quality Assessment.** The characterization of the biodiesel stock solution was performed according to the ASTM 6751 and EN 14214 standards.[17,18]

**2.8. Adsorbent Characterization.** The adsorbents were characterized by means of nitrogen adsorption at −194.6 °C. Before adsorption, the samples were degassed in vacuo at 150


dx.doi.org/10.1021/ef401410v | Energy Fuels 2013, 27, 6763−6772

°C for 2 h. Total pore volume, Brunauer–Emmett–Teller (BET) specific surface area, and pore size distribution [Barrett–Joyner–Halenda (BJH) type] were measured in a Micromeritics apparatus. Thermogravimetric analysis (TGA) of the adsorbents was performed with a Shimadzu TG-1000 instrument. The samples were tested without previous treatment and were considered to be in equilibrium with room humidity.

## 3. RESULTS AND DISCUSSION

Table 1 lists the main properties of the biodiesel base stock. The supercritical transesterification reaction employed produced an increase in the value of free acidity from 0.14% (starting soy oil) to 1.5% (biodiesel). The latter value is higher than the standard limit (0.27%). The experimental water content (450 ppm) was near the standard limit (500 ppm). Therefore, the refining procedure should adjust the acidity level while decreasing the water content or keeping it constant.

**3.1. Screening of Best Adsorbents.** A first round of tests was performed to select a subset of the best performing adsorbents. First, the adsorbents were characterized by means of nitrogen adsorption to assess the surface area and pore volume available for adsorption. The results can be seen in Table 2 and Figure 1. Wheeler's diameter is larger than that

**Table 2. Textural Properties of the Tested Adsorbents[a]**

| adsorbent | Wheeler's $r_p$ (nm) | BET $S_g$ ($m^2\ g^{-1}$) | $V_g$ ($cm^3\ g^{-1}$) |
|---|---|---|---|
| TriSyl 3000 | 3.56 | 631 | 1.12 |
| TriSyl 450 | 3.34 | 597 | 1.00 |
| TriSyl 300B | 3.69 | 592 | 1.09 |
| activated carbon (VAC) | 1.67 | 641 | 0.37 |
| diatomaceous earth (DE) | 2.56 | 169 | 0.22 |

[a] $r_p$: pore radius; $S_g$: specific surface area; $V_p$: pore volume.

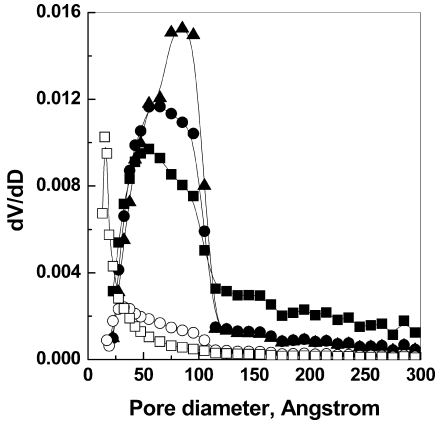


**Figure 1.** Pore size distributions of the tested adsorbents: (▲) TriSyl 300B, (●) TriSyl 450, (■) TriSyl 3000, (○) diatomaceous earth, and (□) activated carbon.

corresponding to the main peak of the pore distribution. This is normal. The two values are expected to coincide only for symmetrical (e.g., Gaussian) distribution curves. The mismatch is especially strong for diatomaceous earth and activated carbon because these adsorbents have relatively narrow peaks in the micropore region and long tails in the meso- and macropore regions. For the silicas, much of the pore volume is associated with mesopores with sizes near the Wheeler's value. The fact that the distribution peaks for diatomaceous earth and activated carbon are in the micropore region indicates that intraparticle pore diffusion resistance is high for these two adsorbents. In fact, the effective size of oleic acid seems sufficiently high, 2 nm, that oleic acid might be unable to reach the micropores of these adsorbents.

The adsorption results in Table 3 partly confirm the previous statements. Activated carbon had the lowest adsorption

**Table 3. Comparative Adsorption Tests of the Studied Materials[a]**

| adsorbent | $\theta$ (min) | $C_{ads}$ (%) | $Q$ (%) |
|---|---|---|---|
| VAC | 160 | 5 | 0 |
| VAC | 720 | 5 | 0.5 |
| IAC | 160 | 5 | 0.9 |
| IAC | 720 | 5 | 1.7 |
| DE | 90 | 0.4 | 3.9 |
| TriSyl 3000 | 90 | 0.4 | 10 |
| TriSyl 450 | 90 | 0.4 | 6.1 |
| TriSyl 300B | 90 | 0.4 | 5.8 |

[a] IAC, impregnated activated carbon; VAC, virgin activated carbon; DE, diatomaceous earth; $\theta$, bleaching time; $C_{ads}$, adsorbent concentration; $Q$, adsorption capacity. Adsorption conditions: 25 °C, atmospheric pressure.

capacity (both VAC and IAC). The silicas showed the best results (adsorption on a mass basis), whereas the results for diatomaceous earth were intermediate. On a surface basis, the loading of adsorbate per unit area was higher for DE (almost 50% higher than for TriSyl 3000), a fact that is likely related to the high polarity of DE. Generally, the adsorption of surfactants from nonpolar media is enhanced with increased polarity of the adsorbent surface. In agreement with this general rule, carbon demonstrated the lowest adsorption capacity. For carbons, Mg leaching was considered to be negligible because such behavior was not reported in other works.[15]

With respect to the error in the data, triplicates of the adsorption tests (90 min, 25 °C, Table 3) for the TriSyl 3000 and 300B silicas gave error estimates for $Q$ of 6.7% and 5.8%, respectively.

As the adsorption capacity on a mass basis was higher for the silicas, only the silicas were considered in the rest of the work.

**3.2. Influence of Bleaching Conditions.** Table 4 contains data from adsorption tests performed at varying conditions of

**Table 4. Influence of Bleaching Conditions on the Adsorption Capacities ($Q$) of the Silicas**

| $T$ (°C) | vacuum | $\theta$ (min) | silica | $W_0$ (%) | $W_f$ (%) | $Q$ (%) |
|---|---|---|---|---|---|---|
| 70 | no | 90 | 3000 | 0.057 | 0.094 | 43 |
| 70 | yes | 90 | 3000 | – | – | 99.3 |
| 70 | yes | 90 | 300B | – | – | 82.0 |
| 70 | yes | 90 | 450 | – | – | 81.0 |
| 90 | yes | 90 | 3000 | – | – | 81.5 |
| 90 | yes | 90 | 300B | – | – | 75.3 |
| 90 | yes | 90 | 450 | – | – | 72.5 |
| 110 | yes | 90 | 3000 | – | – | 75.0 |
| 110 | yes | 90 | 300B | – | – | 69.0 |
| 110 | yes | 90 | 450 | – | – | 63.2 |
| 110 | no | 90 | 3000 | 0.060 | 0.140 | 24 |

$C_{ads}$, adsorbent concentration (0.4%); $W_0$ and $W_f$, initial and final water contents (mass basis), respectively. Abbreviations as in Table 3.


dx.doi.org/10.1021/ef401410v | Energy Fuels 2013, 27, 6763–6772

contact time, temperature, and vacuum level. As can be seen, the influence of adsorption temperature is only secondary, whereas the vacuum level and type of adsorbent are the most important variables.

In the absence of a vacuum, adsorption is very low, 1 order of magnitude lower than the value obtained at 160 mmHg. The reason becomes straightforward from the TGA results of Figure 2. Water adsorption seems to inhibit diffusion and adsorption

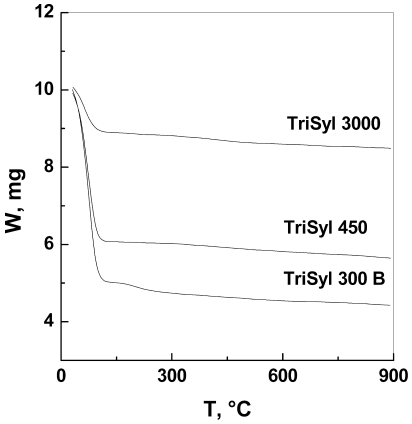


**Figure 2.** TGA traces of the silicas under study.

inside the silica pore networks. At temperatures of 90 °C or higher, water desorption from the adsorbent dipped in oil should proceed rather slowly and is possible only in a vacuum. If the adsorbent is not previously dehydrated, dehydration would occur simultaneously with adsorption during bleaching. In some cases, the release of water from the silica would go directly into the oil phase, thus increasing the biodiesel water content (first and last rows of Table 4, silica TriSyl 3000 at 70 and 110 °C).

For the same adsorbent and in the presence of a vacuum, the influence of temperature is lower than in experiments at atmospheric pressure. For example, for TriSyl 3000 in vacuo, after 90 min from a similar initial acidity level (1.5%), the adsorbate loadings at two different temperatures are $Q_{70\ °C}$ = 99.3% and $Q_{110\ °C}$ = 75.0%. This is a 25% decrease. For TriSyl 3000 at atmospheric pressure, the decrease is 44% for the same temperature change.

Similarly, for TriSyl 300B, at a 90-min bleaching time, for 1.7−1.9% initial acidities, the values are $Q_{70\ °C}$ = 82.0% and $Q_{110\ °C}$ = 69.0%. The trend is clear and indicates that the adsorption equilibrium is not favored by an increase in temperature. This is most probably related to the exothermicity of adsorption.

Adsorption should therefore be performed at a low temperature from a thermodynamic point of view, although high temperatures are needed to make water desorption from the adsorbent surface possible.

In regard to the bleaching time, values of 90−120 min are seemingly necessary to achieve total saturation of the adsorbent. This seems too long if reaction times are kept lower than 90 min. One solution would be to increase the throughput of the bleaching section by adding more bleaching tanks. We will analyze this issue in the next sections.

**3.3. Calculation of the Heat of Adsorption and Henry's Constant for Adsorption.** The equilibrium adsorbate loading, $Q_e$, could be modeled using the Langmuir isotherm

$$Q_e = \frac{Q_m LC}{1 + LC} \tag{1}$$

where $L$ is the Langmuir constant for adsorption and $Q_m$ is the maximum adsorption capacity (in grams of adsorbate per gram of adsorbent). $C$ is the concentration of adsorbate in the liquid phase (in grams of oleic acid per gram of solution). The equilibrium could also be modeled using the Freundlich isotherm equation. The Langmuir formula, however, has been found to better predict the adsorption of impurities in biodiesel on silicas.[19] Nawar and Han[20] also concluded that the Langmuir isotherm is followed by octanoic acid adsorption on silica. The better adjustment of free acid adsorption by the Langmuir model (in comparison to the Freundlich model) was also reported earlier by Procter and Palaniappan.[21]

For tests performed in the dilute concentration range of oleic acid, the Langmuir model should become approximately linear and coincide with Henry's law for adsorption ($Q_e \approx Q_m LC_{FFA} = HC_{FFA}$), whereas for tests performed at high concentrations, the Langmuir formula should reduce to the irreversible square isotherm ($Q_e \approx Q_m$).

Data in the dilute region can be found in our and other reports, for example, that of Sohling et al.[22] on the refining of biodiesel with silica. Taking the linear isotherm approximation, $H$ = 44.6 at 70 °C (TriSyl 3000, Figure 3). $H$ is dimensionless

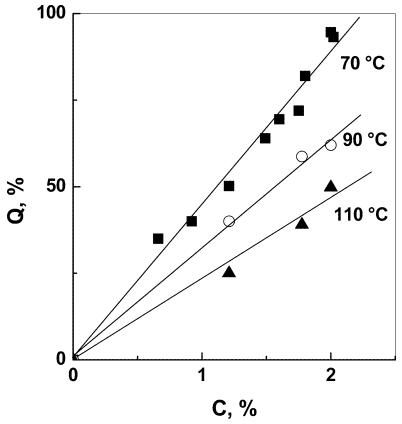


**Figure 3.** Equilibrium adsorption isotherms for TriSyl 3000 silicas at three different temperatures: (■) 70, (○) 90, and (▲) 110 °C. Results previously presented in an adsorption review.[23]

because both the adsorbate loading and the acidity are expressed in terms of weight percentage. $H$ = 18.3 and 31.4 for the same silica at 110 and 90 °C, respectively. It can be noted from these results that the Henry's constant for adsorption is decreased at higher temperatures. This must be related to the exothermicity of adsorption. According to the van't Hoff's rule

$$\frac{d(\ln K)}{d(1/T)} = \frac{-\Delta H}{R} \tag{2}$$

where $K$ is the equilibrium constant, $T$ is the temperature (in kelvin), $\Delta H$ is the heat of adsorption, and $R$ is the ideal gas constant.

Fitting the data with the previous equation, a value for the heat of adsorption of −5.7 kcal mol$^{-1}$ was found. This is almost twice the value found by other researchers for the heat of adsorption of stearic acid on kaolinite, −2.92 kcal mol$^{-1}$.[24]


dx.doi.org/10.1021/ef401410v | Energy Fuels 2013, 27, 6763−6772

**3.4. Theoretical Estimation of the Global Adsorption Rate Coefficient.** Adsorption models are needed for the design of industrial bleachers. From a phenomenological point of view, the process starts in the fluid phase with oleic acid moving from the bulk of the biodiesel solution into the film surrounding the adsorbing particle. A first mass-transfer resistance is found there, with the mass-flux resistance being inversely proportional to the film coefficient $k_f$

$$\frac{\partial Q}{\partial t} = \frac{3k_f}{R_p\rho_p}(C - C_S) \tag{3}$$

$$Q_S = Q_e(C_S) \tag{4}$$

where $C_S$ is the concentration of adsorbate at the liquid−solid interface, in equilibrium with the surface $Q_S$ value, given by the Langmuir or Freundlich isotherm formulas. $R_p$ is the particle radius, and $\rho_p$ is the particle density.

Inside the adsorbent particle, the adsorbate molecules must diffuse through the pore structure, with diffusion represented by Fick's law

$$\frac{\partial Q}{\partial t} = D_e\left(\frac{\partial^2 Q}{\partial r^2} + \frac{2}{r}\frac{\partial Q}{\partial r}\right) \tag{5}$$

If there is no interaction between the diffusing adsorbate and the solid surface, the effective diffusivity should be similar to the molecular diffusivity, $D_{AB}$. In the case of liquid adsorption, the movement of the adsorbate is sometimes dominated by the surface diffusivity ($D_S$), which can be many orders of magnitude smaller than the molecular diffusivity. For example, Yang et al.[25] measured the surface diffusivity of stearic acid over alumina and found that, when the alumina surface was free of coadsorbed water, the diffusivity was equal to $2 \times 10^{-11}$ m$^2$ s$^{-1}$, whereas it was $4 \times 10^{-9}$ m$^2$ s$^{-1}$ when the surface was covered with water.

To check the importance of all resistances in the adsorption mechanism, the film coefficient and the intraparticle diffusivity should be estimated. The molecular self-diffusivity of oleic acid was calculated as $5 \times 10^{-11}$ m$^2$ s$^{-1}$.[26] The diffusivity of oleic acid in nut oil was measured at 130 °C and found to be $4.2 \times 10^{-10}$ m$^2$ s$^{-1}$.[27] Using the Wilke−Chang equation,[28] the diffusion constant of oleic acid in methyl oleate can be estimated as

$$D_{AB} = \frac{7.4 \times 10^{-12}(\phi_B M_B)^{1/2}}{\mu_B V_A^{0.6}} \tag{6}$$

where A represents oleic acid, B represents methyl oleate, $M_B$ = 296.5 g mol$^{-1}$, $V_A$ = 317.8 cm$^3$ mol$^{-1}$, $\phi_B$ = 1.5 (association factor), $T$ = 363 K, and $\mu$ = 4 mPa s. With these values, $D_{AB}$ = $4.46 \times 10^{-10}$ m$^2$ s$^{-1}$ (similar to the values reported elsewhere).[29]

The film coefficient can be estimated with the aid of a correlation for mass transfer in suspension reactors[30]

$$Sh^2 = 4 + 1.21Pe^{2/3} \tag{7}$$

$$\left(\frac{k_f d_p}{D_{AB}}\right)^2 = 4 + 1.21\left(\frac{d_p u}{D_{AB}}\right)^{2/3} \tag{8}$$

In eq 8, $d_p$ is the particle diameter. The solid−fluid velocity $u$ varies little with the stirring rate, which is why $k_f$ for stirred tanks is not highly dependent on the stirrer Reynolds number. A common solid−fluid velocity for small particles and high stirring rates is 10 cm s$^{-1}$. Adopting this value for $u$ and recalling that $d_p$ = 74 $\mu$m (200 US mesh), the value of $k_f$ from eq 8 is $k_f = 1.7 \times 10^{-4}$ m s$^{-1}$.

An overall mass-transfer coefficient, $K$, can be obtained from an equation due to Ruthven et al.[31]

$$\frac{1}{K} = \frac{R}{3k_f} + \frac{R^2}{15\varepsilon D_{AB}} \tag{9}$$

$$\frac{1}{K} = 0.073\ \text{s} + 0.341\ \text{s} \approx 0.4\ \text{s}$$

$\varepsilon$ is the porosity of the adsorbent particle (0.5−0.6 for TriSyl silicas). The result indicates that, during refining with silica powders, the mass-transfer mechanism should be controlled by intraparticle diffusion and that the liquid−solid mass-transfer resistance is of minor importance.

However, there still remains the question of whether adsorption kinetics plays any role. During adsorption and after the molecule has trespassed the film surrounding the particle and also diffused into the porous channels of the sorbent, the adsorption rate for a molecule of adsorbate should be similar to that of a chemical reaction with the solid. Several models have been suggested for adsorption, many of them only empirical. The following equation are taken from the review of Ho et al.[32]

Zeroth-order reaction

$$Q(t) = Q_0 + k_0 t \tag{10}$$

First-order reaction

$$\ln[Q(t)] = \ln[Q_0] + k_1 t \tag{11}$$

Second-order reaction

$$\frac{1}{Q(t)} = \frac{1}{Q_0} + k_2 t \tag{12}$$

Third-order reaction

$$\frac{1}{[Q(t)]^2} = \frac{1}{Q_0^2} + k_3 t \tag{13}$$

Parabolic diffusion

$$Q(t) = \alpha + k_d t \tag{14}$$

Elovich-type equation

$$Q(t) = Q_0 + \frac{1}{\beta}\ln(\alpha\beta) + \frac{1}{\beta}\ln(t) \tag{15}$$

In the review of Ho et al.,[32] results related to adsorption on clays and silicas are reported to be well represented by the model of the first-order reaction. These results include Ni(II) adsorption on wollastonite, Ni(II) on China clay, Pb(II) on kaolinitic clay, and Hg(I) on kaolinite. The same occurs for F, P, and As(V) adsorption on silica, as well as lactoglobulin and hemoglobin adsorption on silica.

Equations 10−15 do not take into consideration the limitation of the finite equilibrium capacity of adsorption of the solid. To overcome this limitation, some other models have been proposed. For example, the pseudo-second-order model was proposed by Ho and McKay[33] and is suggested to better fit the data for some systems previously reported to be described by first-order adsorption kinetics.


dx.doi.org/10.1021/ef401410v | Energy Fuels 2013, 27, 6763−6772

Pseudo-second-order model

$$\frac{dQ}{dt} = k(Q_e - Q)^2 \quad (16)$$

However, the most popular model including kinetics, mass-transfer limitations, and equilibrium limitations is the linear-driving-force (LDF) model[34]

Linear-driving-force model

$$\frac{dQ}{dt} = K(Q_e - Q) \quad (17)$$

In both eqs 16 and 17, $Q_e$ is the equilibrium concentration of adsorbate on the solid. Depending on the concentration range studied, $Q_e$ can be written as a Langmuir trace (eq 1, full range), a constant ($Q_e = Q_m$, saturation range), or a linear trace ($Q_e = HC$, high dilution range).

Equation 9 is usually used to estimate $K$ in cases where the system is dominated by mass-transfer limitations. In this work, the LDF model was used to correlate the experimental data of fatty acid adsorption on silica.

**3.5. *H* and *K* Parameters for the LDF Model.** Taking $H$ = 44.6, we used the linear isotherm equation and the LDF kinetic equation to fit the data of Figure 4. Because the system of the experiment is closed, a mass balance must be made to account for the exchange of adsorbate between the solid and liquid phases. The final equations are

$$\frac{dQ}{dt} = K(HC - Q) \quad (18)$$

$$\frac{dC}{dt} = -\alpha \frac{dQ}{dt} \quad (19)$$

In eq 19, $\alpha$ is the concentration of adsorbent (in $g_{ads}\ g_{sol}^{-1}$). For the system at 70 °C, $K_{70\ °C}$ = 0.0352 $min^{-1}$. The fitted value of $K$ is almost 4 orders of magnitude smaller than that predicted from our previous calculations based on molecular diffusivity, for a system dominated by intraparticle diffusion. This could be due to two reasons: (i) The intraparticle effective diffusivity is controlled not by molecular diffusivity but by much slower surface diffusion phenomena, with values of surface diffusivity as small as $10^{-15}$ $m^2\ s^{-1}$. (ii) The intrinsic adsorption kinetics are even slower than the adsorbate diffusion rates, with values of the rate constant as low as $k$ = 0.03 $min^{-1}$.

In the case of reason i, it must be recalled that, after the adsorbates pass through the hydrodynamic boundary layer, they are transported through the pores of the adsorbent to the available adsorption sites by intraparticle transport involving either molecular diffusion through the solution in the pores (pore diffusion) or diffusion along the adsorbent surface (surface diffusion). Then, adsorption takes place over the available sites. Surface diffusion takes place by "hopping" of the molecules from one adsorption site to another and is a slow process. For example, in the case of activated carbons, both the "pore volume diffusion model" (PVDM) and the "surface diffusion model" (SDM) have been used to predict the diffusion of aromatic dyes inside carbon particles.[35] These authors found that the contribution of surface diffusion to the overall intraparticle diffusion was 82% for phenol and 19% for methyl blue. The mass-transfer resistance in the external boundary layer was negligible.

Fitting the same model for adsorption data at the other two temperatures (see Figure 4) leads to even lower values of the global mass-transfer coefficient ($K_{90\ °C}$ = 0.0188 $min^{-1}$, $K_{110\ °C}$ = 0.013 $min^{-1}$). Figure 5 shows the results of adsorption as a function of time for silica TriSyl 300B. Fitting the data yields $K_{70\ °C}$ = 0.032 $min^{-1}$, $K_{90\ °C}$ = 0.022 $min^{-1}$, and $K_{110\ °C}$ = 0.018 $min^{-1}$ (kinetics experiments); $H_{70\ °C}$ = 33.2, $H_{90\ °C}$ = 30.4, and $H_{110\ °C}$ = 27.1 (equilibrium adsorption). (These $K$ values were included in a previous review on adsorption[23] to show the slow kinetics of FFA adsorption.)

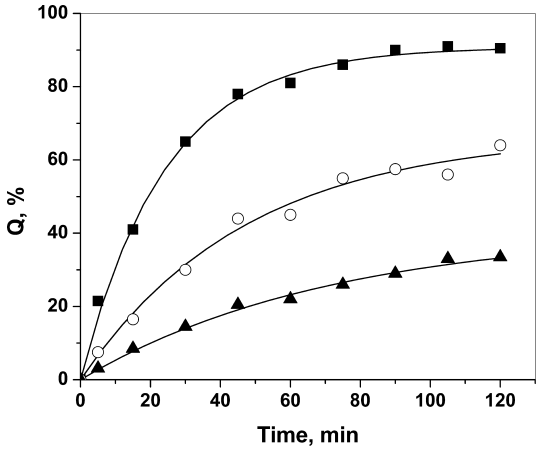


**Figure 4.** Adsorption kinetics. Tests with TriSyl 3000 silica at three different temperatures: (■) 70, (○) 90, and (▲) 110 °C. Adsorbent concentration, 0.4%; initial biodiesel acidity, 2.4%; vacuum pressure, 160 mmHg.

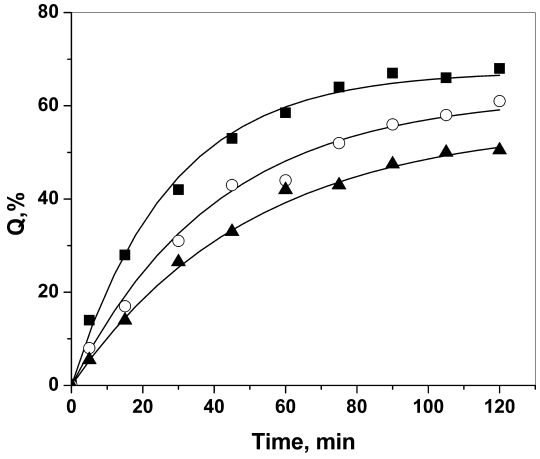


**Figure 5.** Adsorption kinetics. Tests with TriSyl 300B silica at three different temperatures: (■) 70, (○) 90, and (▲) 110 °C. Adsorbent concentration, 0.4%; initial biodiesel acidity, 2.3%; vacuum pressure, 160 mmHg.

The decrease in the value of $K$ at higher temperatures is difficult to explain, as both the intrinsic adsorption kinetic rate and the mass-transfer coefficients should increase with temperature. One possible explanation is that some hydrolysis of fatty acid methyl esters (FAMEs) on silica occurred during the experiments and that this effect was more pronounced at higher temperatures. In any case, the goodness of fit indicates that the system can be well described by a linear-driving-force model.

**3.6. *Q* as a Function of the Adsorbent Hydration Degree.** At 90 min. both silicas have much lower $Q$ values for similar amounts of free fatty acids in solution at the beginning


dx.doi.org/10.1021/ef401410v | Energy Fuels 2013, 27, 6763−6772

of the test. An important factor for the lower adsorption capacity of these silicas can be seen in Figure 2. This figure contains the TGA traces of the three silicas under study. At temperatures near 40 °C, a great loss of mass begins for all three silicas that is finished at about 110−120 °C. The higher mass loss occurs on the TriSyl 450 and 300B samples. This loss is attributed to the release of adsorbed water. This water would interfere with the adsorption of FFAs because water molecules block adsorption sites.

Most modern bleaching apparatuses are designed to operate under a vacuum to take advantage of the beneficial effect of oxygen exclusion. Oxygen is to be excluded to prevent oil oxidation at the high temperatures of bleaching. The oil is usually cooled either before filtration or at the discharge of a filter to prevent exposure of hot oil to the atmosphere. The results indicate that, for biodiesel refining with silicas, an additional benefit coming from the vacuum treatment is the enhancement of the adsorption capacity.

**3.7. Influence of the Bleaching Time on the Final Water Content of Biodiesel.** As previously stated, the bleaching procedure should adjust the acidity level while decreasing or not modifying the water content. Figure 6 shows the water content as a function of bleaching time for the three silicas. In all three cases, the bleaching treatment does not increase the biodiesel water content.

**3.8. Simulation of Serial Biodiesel Bleaching Units.** An important advance in bleaching technology has been the development of continuous processing systems. Some of these systems operate in a countercurrent pattern for the oil and adsorbent streams, usually employing two stages. The Öhmi process uses two bleaching columns, two filter units, and recycling of the spent bleaching earth from the second column to the first one.[36] Both laboratory research and pilot-plant studies have shown that approximately 40% of the bleaching earth is saved by using the countercurrent bleaching principle and a setup of two serial bleaching units. The working principle is that adsorbent that has reached equilibrium with respect to the adsorbing power of impurities with the effluent oil still has bleaching power for the more contaminated unbleached oil and then the staged countercurrent addition of bleaching earth results in a saving of bleaching earth (see Figures 7 and 8). This principle was previously applied in a rudimentary way in the Votator system, using the filter press with spent bleaching earth as the adsorption unit.[37] In Figure 7, the line labeled 1 is the operation line for a one-unit bleaching operation. The line labeled 2 is the operation line for a countercurrent two-unit bleaching operation. The solid main line is the equilibrium isotherm of the adsorbent. The c.c. line is the ideal operation line for an infinite number of countercurrent stages. $1/\alpha$, the inverse of the slope of the operation line, is related to the bleaching earth dosing (consumption). Clearly, the two-unit countercurrent operation results in a lower consumption of bleaching earth while reaching the same final adsorbate concentration in the fluid phase.

One aspect not included in Figure 7 is that of the operation time. The $Q$ versus $C$ plot is an equilibrium line, and points on this line could possibly not be reached in a reasonably short time. This could be the case for FFA adsorption on silica. The slow uptake of FFA by silica could lead to two negative consequences: (i) If a high level of FFA removal and a short bleaching time are required, then large amounts of adsorbent should be used, and the adsorbents would become only partially used. (ii) If total utilization of the adsorbent is desired,

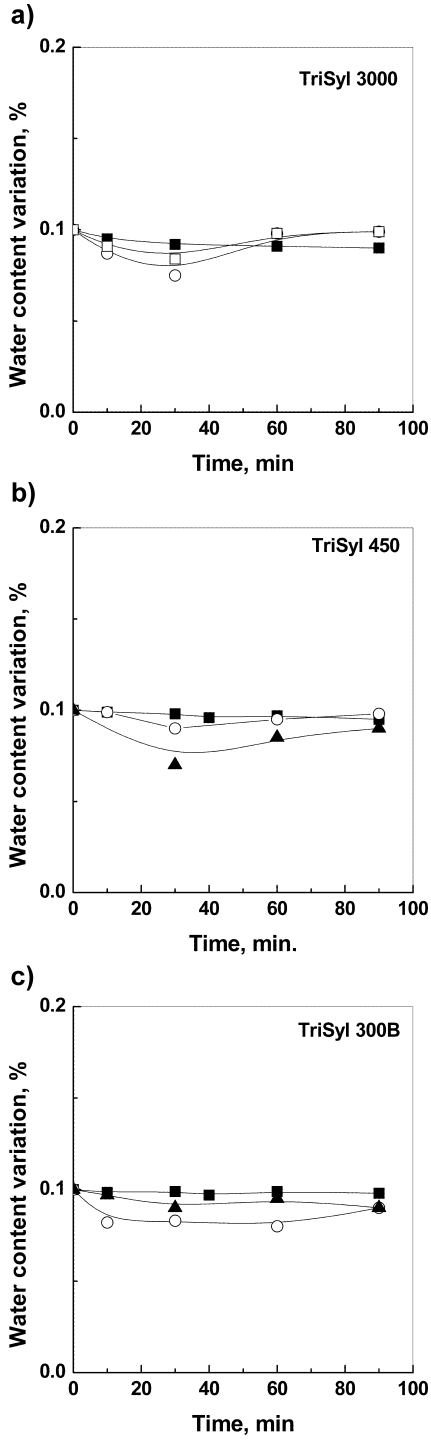


**Figure 6.** Water content as a function of time at (■) 70, (○) 90, and (▲) 110 °C for (a) TriSyl 3000, (b) TriSyl 450, and (c) TriSyl 300B silicas. Vacuum pressure, 160 mmHg.

inconveniently high bleaching times would be necessary. It seems therefore convenient to determine and compare the conditions for high adsorbent utilization and for quasicomplete FFA removal and, most important, to determine how much a countercurrent bleaching system can improve the bleaching earth consumption. This was done by simulation using the equilibrium and mass-transfer parameters for the TriSyl 3000 material. The adsorption process variables and parameters used were as follows: temperature = 90 °C, pressure = 160 mmHg, $K$


dx.doi.org/10.1021/ef401410v | Energy Fuels 2013, 27, 6763−6772

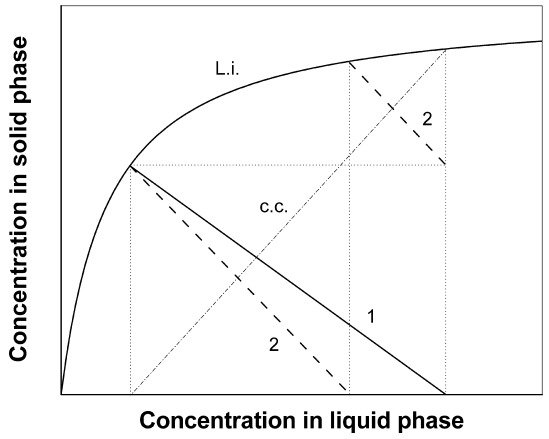


**Figure 7.** Bleaching earths savings in countercurrent bleaching.[32] L.i., equilibrium isotherm; 1, one-bleacher operation line; 2, two-bleacher countercurrent operation line; c.c., continuous countercurrent operation line.

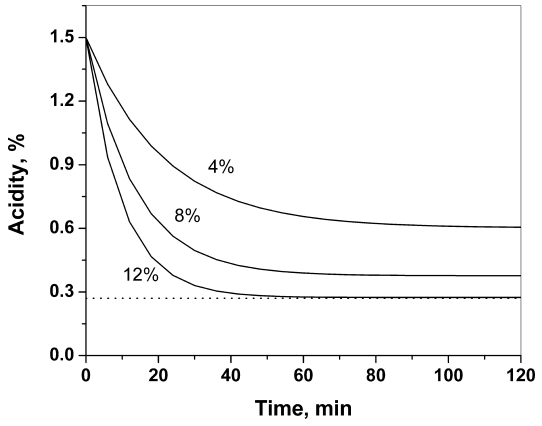


**Figure 9.** Biodiesel acidity as a function of bleaching time. One bleaching unit and different adsorbent loadings, $C_0$ = 1.5%. Dotted line: European standard EN 14214 limit.

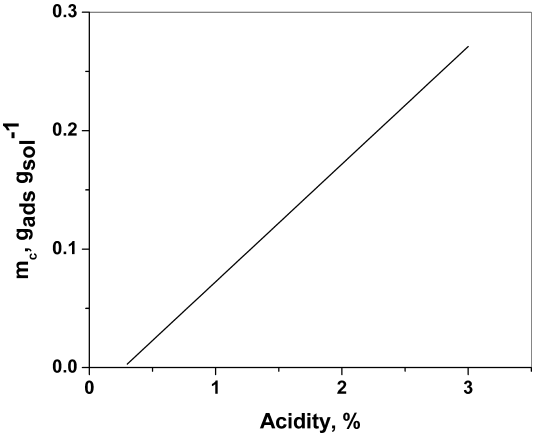


**Figure 10.** Adsorbent concentration needed to obtain a final acidity value corresponding to the EN 14214 limit. Adsorbent concentration as a function of initial biodiesel acidity in a single bleaching unit. Thermodynamic equilibrium is assumed.

= 0.0188 $min^{-1}$, $H$ = 37.3. Equations 18 and 19 were used. These equation can be used for both discontinuous tank bleachers and continuous column bleachers provided that the tank bleaching time is made equal to the column residence time and plug flow is assumed for both earth and oil in the column. The $K$ parameter obtained experimentally in the laboratory stirred-tank reactor is considered to be representative of the mass transfer in the industrial units (large stirred tank for discontinuous bleaching; agitated tower for continuous bleaching).

Biodiesel synthesized in supercritical reactors has a residual FFA content of about 1.5−2.5%.[7] A target maximum FFA content of 0.5 mg of KOH per gram of oil (as measured by ASTM D 664, EN 14104, or a similar method) is desired, which is equivalent to 0.27% FFA (grams of oleic acid per 100 g of biodiesel). Figure 9 contains the results of the simulation of a bleacher performing the acidity adjustment of biodiesel with 1.5% acidity, a typical product of a transesterification reactor using the supercritical method. It can be seen that large amounts of silica are needed to adjust the acidity to reasonable values and that reaching equilibrium takes a fairly long time. The thermodynamic adsorption equilibrium is practically attained at 90 min for the system with 4% loading (4 g of adsorbent per 100 g of solution) and at 60 min for the system with 12% silica. Figure 10 contains a plot of the adsorbent concentration needed in a single bleacher for achieving a final concentration value equal to the EN 14104 limit. This plot assumes thermodynamic equilibrium and was obtained by solving the mass balance between the solid and fluid phases

$$C_0 - C_f = m_c(Q_0 - Q_f) \quad (20)$$

with attention to the adsorption equilibrium ($Q = HC$). $C$ is the concentration of FFA in the liquid phase and $Q$ the concentration of FFA in the solid phase. The subscripts 0 and f indicate the initial and final states, respectively.

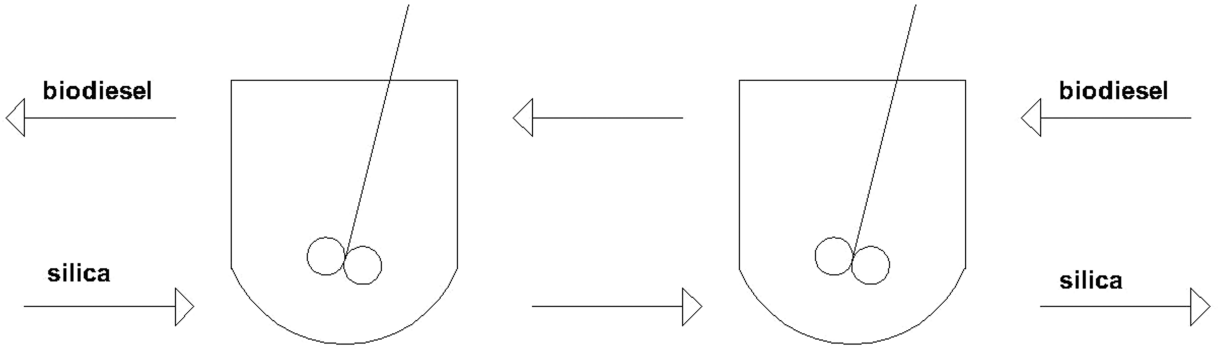


**Figure 8.** Scheme of a serial countercurrent bleaching operation with two bleaching tanks.


dx.doi.org/10.1021/ef401410v | Energy Fuels 2013, 27, 6763−6772

It can be seen that the plot in Figure 10 is linear and that the adsorbent concentration is prohibitively large even at moderate acidity values. The high silica loading in the one-bleacher operation points to the possible use of countercurrent bleaching. Figure 11 is the results of simulations of one, two, and three bleachers in series treating a biodiesel with 1.5% acidity. The adsorbent concentration was 4% (grams of solid per 100 g of solution) in every bleacher. The total bleaching time was the same for every configuration, for example, 120 min for the single bleacher and 40 min for every unit of the three-bleacher setup. The simulation results indicate that, with this adsorbent concentration, it is impossible to achieve the EN 14104 limit with one bleacher, even at long reaction times. It is possible, however, to reach this limit using three bleachers in series with countercurrent flow of the adsorbent. The minimum adsorbent concentration is 12% for the single bleacher and 4% for the serial setup with three units.

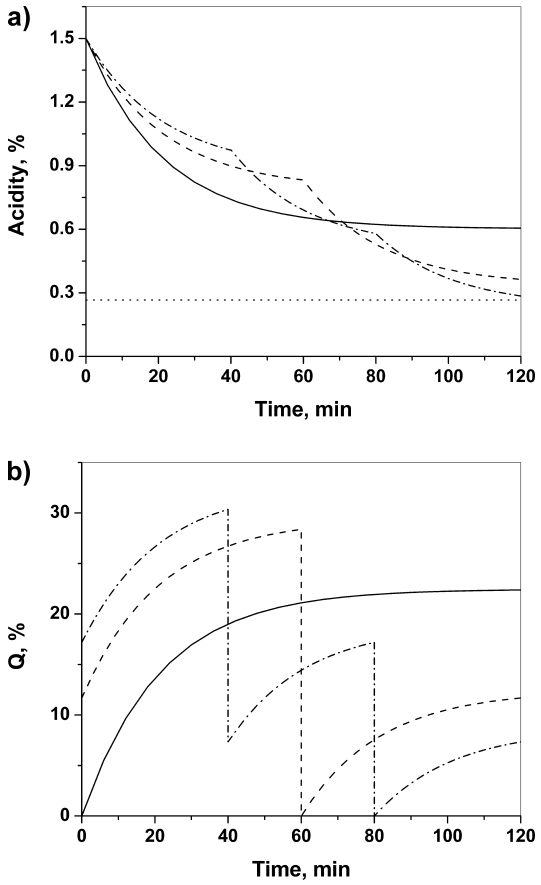


**Figure 11.** (Top) Biodiesel acidity as a function of time and number of bleaching units. (Bottom) Adsorbent loading as a function of time and number of bleaching units (the common time line is that of the oil phase). Adsorbent concentration, 4%. Solid line, one unit; dashed line, two units; dash-dotted line, three units; dotted line, EN 14214 limit.

The comparison of the one-bleacher and three-bleacher setups indicates that, for the same total bleaching time, the single bleacher achieved equilibrium whereas equilibrium was not attained in any of the units of the serial setups. Nevertheless, the final value of Q is 20% in the one-bleacher system and 30% in the three-bleacher system.

It can also be seen that there is a large improvement when going from the single bleacher to the two-unit setup but that this improvement is smaller when comparing two and three units in series. There is therefore a trade-off between the cost of installation of a higher number of units and the savings of spent adsorbent when operating the system. The current results on the convenience of countercurrent bleaching rectify our previous conclusions on this issue.[23]

The a priori destination of the spent silica adsorbent would be the repository of solid effluents of the plant. This is the case for spent bleaching clays used in edible oil refining. Spent bleaching clays can be regenerated by thermal or chemical treatments, but these can be complex or deleterious to the clay structure.[38−40] Conversely, Yori et al.[14] reported the regeneration of spent silica used for deglycerolization of biodiesel by simple flushing with methanol. Further research is clearly needed to assess the regenerability of silicas spent during the adsorption of free fatty acids.

## 4. CONCLUSIONS

Biodiesel streams with up to 2% FFA contents can be efficiently refined by adsorption with silica. In this sense, the use of noncatalytic reaction units, the suppression of washing steps, and the use of adsorption for the refining steps leads to a process that can be carried out under completely "dry" conditions.

Amorphous silica gels of the TriSyl type are excellent adsorbents for FFAs in biodiesel, with a capacity of adsorption of up to 100% (weight/weight). Their capacity for adsorption is much higher than that displayed by virgin and impregnated activated carbons or diatomaceous earth. This is attributed to the uniform mesoporous distribution of the silicas and their polar surface.

Adsorption of FFAs onto TriSyl silicas displays a linear isotherm in the range of interest for biodiesel acidity adjustment (0−3%). The measured heat of adsorption is about −5.7 kcal $mol^{-1}$.

The adsorption kinetics of biodiesel FFAs over the silica surface are very slow despite the use of powdery adsorbents. This indicates that either the intrinsic kinetics are slow or the process is dominated by slow intraparticle mass-transfer resistance.

The adsorption on TriSyl silicas is highly dependent on their hydration degree. All bleaching operations should therefore be performed in vacuo at temperatures in the range of 70−90 °C. Vacuum would remove water blocking adsorption sites and would also remove oxygen to prevent the oxidation of the biodiesel. Silica bleaching adjusts the biodiesel acidity level without adversely modifying the water content.

In adsorbent−adsorbate closed systems with linear isotherms, the adsorbent concentration needed to produce a specific final value of adsorbate concentration in the liquid phase is a linear function of the initial acidity of the solution. In the silica−FFA system, the slope of the line is quite low and dictates a high adsorbent consumption if a single bleacher is used.

The use of serial bleachers in countercurrent mode greatly improves the economy of the process in the silica−FFA system. For an initial biodiesel acidity of 1.5% and a final value of 0.27% (quality standard value), a system with three bleachers in series needs about one-third the amount of adsorbent needed by a single-bleacher system (the biodiesel−silica contact time for each serial bleacher is one-third the bleaching time of the single bleacher; the total process time is the same).


dx.doi.org/10.1021/ef401410v | Energy Fuels 2013, 27, 6763−6772

## AUTHOR INFORMATION


### Corresponding Author

*Tel.: +54-324-4533858. E-mail: cvera@fiq.unl.edu.ar.


### Notes

The authors declare no competing financial interest.

## ACKNOWLEDGMENTS

This research was sponsored by the Argentina National Research Council (CONICET, PIP Grant 0398) and Universidad Nacional del Litoral (CAI+D Grants 60-299 and 60-298).

## REFERENCES


(1) Kafuku, G.; Mbarawa, M. Alkaline catalyzed biodiesel production from moringa oleifera oil with optimized production parameters. *Appl. Energy* **2010**, *87*, 2561−2565.

(2) Freedman, B.; Pryde, E.; Mounts, T. Variables affecting the yields of fatty esters from transesterified vegetable oils. *J. Am. Oil Chem. Soc.* **1984**, *61*, 1638−1643.

(3) Liu, K. Preparation of fatty acid methyl esters for gas-chromatographic analysis of lipids in biological materials. *J. Am. Oil Chem. Soc.* **1994**, *71*, 1179−1187.

(4) Mittelbach, M.; Pokits, B.; Silberholz, A. Diesel fuel derived from vegetable oils, IV: Production and fuel properties of fatty acid methyl esters from used frying oil. In *Proceedings of the 1992 Alternative Energy Conference*; American Society of Agricultural Engineers: St. Joseph, MI, Dec 14−15, 1992; p 74.

(5) Montefrio, M. J.; Xinweng, T.; Obbard, J. P. Recovery and pretreatment of fats, oil and grease from grease interceptors for biodiesel production. *Appl. Energy* **2010**, *87*, 3155−3161.

(6) Balat, M.; Balat, H. Progress in biodiesel processing. *Appl. Energy* **2010**, *87*, 1815−1835.

(7) Manuale, D.; Mazzieri, V.; Torres, G.; Vera, C.; Yori, J. Non-catalytic biodiesel process with adsorption-based refining. *Fuel* **2010**, *90*, 1188−1196.

(8) Anitescu, G.; Deshpande, A.; Tavlarides, L. Integrated technology for supercritical biodiesel production and power cogeneration. *Energy Fuels* **2008**, *22*, 1391−1399.

(9) Karaosmanoglu, F.; Cigizoglu, K.; Tuter, M.; Ertekin, S. Investigation of the refining step of biodiesel production. *Energy Fuels* **1996**, *10* (4), 890−895.

(10) Leung, D. Y. C.; Wu, X.; Leung, M. K. H. A review on biodiesel production using catalyzed transesterification. *Appl. Energy* **2010**, *87*, 1083−1895.

(11) Clowutimon, W.; Kitchaiya, P.; Assawasaengrat, P. Adsorption of free fatty acid from crude palm oil on magnesium silicate derived from rice husk. *Eng. J.* **2011**, *87*, 15−25.

(12) Maddikeri, G. L.; Pandit, A. B.; Gogate, P. R. Adsorptive removal of saturated and unsaturated fatty acids using ion-exchange resins. *Ind. Eng. Chem. Res.* **2012**, *51*, 6869−6876.

(13) Manuale, D. L. Doctoral Thesis, Universidad Nacional del Litoral, Santa Fe, Argentina, 2010.

(14) Yori, J.; D'Ippolito, S.; Pieck, C.; Vera, C. Deglycerolization of biodiesel streams by adsorption over silica beds. *Energy Fuels* **2007**, *21* (1), 347−353.

(15) Sinha, R. MgO impregnated activated carbon and its use in an improved vegetable oil refining process. U.S. Patent 4,150,045, 1979.

(16) D'Ippolito, S.; Yori, J.; Iturria, M.; Pieck, C.; Vera, C. Deglycerolization of biodiesel streams by adsorption over silica beds. *Energy Fuels* **2007**, *21* (1), 339−346.

(17) ASTM D6751. Standard specification for biodiesel fuel blend stock (B100) for middle distillate fuels. In *Annual Book of ASTM Standards*; American Society for Testing and Materials: Philadelphia, PA, 1999.

(18) *Automotive fuels − Fatty acid methyl esters (FAME) for diesel engines − Requirements and test methods*; Standard EN 14214; Beuth-Verlag: Berlin, Germany, 2012.

(19) Mazzieri, V.; Vera, C.; Yori, J. Adsorptive properties of silica gel for biodiesel refining. *Energy Fuels* **2008**, *22*, 4281−4284.

(20) Nawar, W.; Han, L. Thermal oxidation of lipids in monolayers. I. The nature of binding on silica. *J. Am. Oil Chem. Soc.* **1985**, *62* (11), 1596−1598.

(21) Proctor, A.; Palaniappan, S. Adsorption of soy oil free fatty acids by rice hull ash. *J. Am. Oil Chem. Soc.* **1990**, *67* (1), 15−17.

(22) Sohling, U.; Ruf, F.; Ortiz Niembro, J.; Condemarin, R.; Bello, J. Method for purification of biodiesel. U.S. Patent Application 2010/0132251, 2010.

(23) Vera, C.; Busto, M.; Yori, J.; Torres, G.; Manuale, D.; Canavese, S.; Sepùlveda, J. Adsorption in biodiesel refining: A review. In *Biodiesel: Feedstocks and Processing Technologies*; InTech Open Access Publishers: Rijeka, Croatia, 2011; Chapter 21.

(24) Sari, A.; Ipýldak, Ö. Adsorption properties of stearic acid onto untreated kaolinite. *Bull. Chem. Soc. Ethiop.* **2006**, *20* (2), 259−267.

(25) Yang, R.; Fenn, J.; Haller, G. Surface diffusion of stearic acid on aluminum oxide. *AIChE J.* **1974**, *20* (4), 735−742.

(26) Kraai, G. N.; Winkelman, J. G. M.; de Vries, J. G.; Heeres, H. J. Kinetic studies on the *Rhizomucor miehei* lipase catalyzed esterification reaction of oleic acid with 1-butanol in a biphasic system. *Biochem. Eng. J.* **2008**, *41* (1), 87−94.

(27) Smits, G. Measurement of the diffusion coefficient of free fatty acid in groundnut oil by the capillary-cell method. *J. Am. Oil Chem. Soc.* **1976**, *53* (4), 122−124.

(28) Reid, R.; Prausnitz, J.; Poling, B. *The Properties of Gases and Liquids*, 5th ed.; McGraw-Hill: New York, 2001.

(29) Kimmel, T. Doctoral Thesis, Technischen Universität Berlin, Berlin, Germany, 2004.

(30) Levenspiel, O. *Chemical Reaction Engineering*; John Wiley & Sons: New York, 1972.

(31) Ruthven, D.; Farooq, S.; Knaebel, K. *Pressure Swing Adsorption*; VCH Publishers: New York, 1994.

(32) Ho, Y. S.; Ng, J. C. Y.; McKay, G. Kinetics of pollutant sorption by biosorbents: Review. *Sep. Purif. Methods* **2000**, *29* (2), 189−232.

(33) Ho, Y. S.; McKay, G. *Process Biochem.* **1999**, *34*, 451−465.

(34) Ahn, H.; Lee, C. Effects of capillary condensation on adsorption and thermal desorption dynamics of water in zeolite 13X and layered beds. *Chem. Eng. Sci.* **2004**, *59*, 2727−2743.

(35) Ocampo-Pérez, R.; Leyva-Ramos, R.; Sanchez-Polo, M.; Rivera-Utrilla, J. Role of pore volume and surface diffusion in the adsorption of aromatic compounds on activated carbon. *Adsorption* **2013**, *19*, 945−957.

(36) Transfeld, P. Countercurrent bleaching of rapeseed oil. Presented at the *10th International Rapeseed Congress*, Canberra, Australia, Sep 26−29, 1999.

(37) Singleton, W.; Mc Michael, C. Continuous countercurrent vacuum bleaching. *J. Am. Oil Chem. Soc.* **1955**, *32*, 1−14.

(38) Tsai, W. T.; Chen, H. P.; Hsieh, M. F.; Sun, H. F.; Lai, C. W. Regeneration of bleaching clay waste by chemical activation with chloride salts. *J. Environ. Sci. Health A* **2003**, *38* (4), 685−696.

(39) Boukerroui, a.; Ouali, M.-S. Regeneration of a spent bleaching earth and its reuse in the refining of an edible oil. *J. Chem. Technol. Biotechnol.* **2000**, *75* (9), 773−776.

(40) Chang, J. I.; Tai, H.-S.; Huang, T. H. Regeneration of spent bleaching earth by lye extraction. *Environ. Prog.* **2006**, *25* (4), 373−378.